The impact of turbulence on sediment erosion around submerged aquatic vegetation

Xinya Liang, National University of Singapore, xinya.liang@u.nus.edu
Jiarui Lei, National University of Singapore, jlei@nus.edu.sg

INTRODUCTION

Nature-based solutions provide safeguarding, sustainable governance, and rehabilitation for ecosystems while concurrently offering benefits for human society (Seddon et al., 2020). As a common choice for nature-based solutions, submerged aquatic vegetation (SAV) is ubiquitous and important for coastal and riverine ecosystems due to its ability to reduce flow velocity and dissipate wave energy. Previous research, such as that by Nepf (2012), has examined the velocity profiles related to a submerged canopy that spans the entire width of a channel. In natural environments, SAV often exhibits patchy distributions accompanied by three-dimensional (3-D) velocity fields. Lei and Nepf (2021) provided an analytical flow velocity model for 3-D canopies. Although many studies have confirmed that vegetation patches enhance sediment deposition in the vegetated region (i.e., Kim et al., 2018; Västilä and Järvelä, 2018), how the 3-D canopies impact flow structures and sediment transport remains uncertain. To be more specific, the evolution and mixing processes of the turbulence and its impact on sediment erosion along the 3-D canopies cannot be well described by existing theories. In this study, we aim to disclose the physical mechanisms of flow-vegetation-sediment interaction. Theoretical derivations, laboratory experiments, and large-eddy simulations were combined to investigate the effects of 3-D submerged artificial vegetation on sediment transport and flow development in unidirectional flows.

METHODOLOGY

In our theoretical derivations, we began by analyzing turbulence in fully developed 2-D meadows and then extended the theory to 3-D meadows. For the laboratory experiments, we used a current flume located in the Hydraulic Laboratory at the National University of Singapore. The investigation of 3-D vegetation impacts involved the estimation of hydraulic conditions and vegetation parameters. For the numerical simulations, an in-house code, CgLES-IBM (Complex Geometry Large Eddy Simulation-Immersed Boundary Method), was applied in our study.

THEORETICAL MODELING

Lei and Nepf (2021) proposed a two-layer model to describe the fully developed velocity vertical distribution in 3-D canopies:

$$\frac{U_1}{U_\infty} = \frac{1}{1-\frac{bh}{WH}\phi+\sqrt{\frac{C_D a b h}{2C_{3Dim}(b+h)(1-\phi)}\left(\frac{WH-bh}{WH}\right)^3}} \quad (1)$$

$$U_2 = \frac{U_\infty WH - U_1 bh(1-\phi)}{(WH-bh)} \quad (2)$$

where U_1 is the canopy layer velocity in the fully developed region, U_2 is the overflow layer velocity in the fully developed region, U_∞ is the open-channel flow velocity, W is the channel width, b is the vegetation width, H is the water depth, h is the canopies height, $\phi = \frac{\pi d^2}{4}$ is the solid volume fraction of the canopies, d is the stem diameter, and C_{3Dim} is the modified shear coefficient for 3-D meadows. The vegetation-generated turbulence consists of the stem turbulence production and the shear production. Eq. (8) in Zhang et al. (2020) shows that the stem turbulence production can be expressed as

$$\langle P_{\text{stem}} \rangle = C_{DF}\frac{nd}{2(1-\phi)}U_1^3 \quad (3)$$

Here, the angle brackets denote the within-meadow average, C_{DF} is the form drag coefficient (usually we can assume that $C_{DF} \approx C_D$), and n is the stem density. Following the derivation from Lei and Nepf (2021), the shear production term is modified to

$$\langle P_{\text{shear}} \rangle = \frac{1.3}{\frac{bh}{b+h}}C^{3/2}(U_2-U_1)^3 \quad (4)$$

Combining equations (3) and (4), the turbulent kinetic energy (TKE) can be estimated using the following equation.

$$\langle k_t \rangle = \left(\left(\langle P_{\text{stem}} \rangle + \langle P_{\text{shear}} \rangle\right)\beta d\right)^{2/3} \quad (5)$$

with $\beta = 3.6 \pm 0.6$ a scale factor (Zhang et al., 2020).

LABORATORY EXPERIMENTS

Experiments were conducted in a recirculating flume with the size of $W \times H \times L = 0.6 \times 0.6 \times 15$ m^3. A cycling system equipped with pumps was devised to maintain a consistent flow rate within the flume. By repeated experiments, inlet velocity fluctuations were confirmed to negligibly small when flow rates and water levels in the flume remain the same, which agreed with the findings in Chew et al. (2017).

The vegetation model was fabricated using rigid wooden cylinders with a diameter of 6 mm and a vegetation frontal area per unit meadow volume $a = 2.5$ cm^{-1}. It is both finite in width and height, making the canopies three-dimensional. The model canopies are 20 cm high (8 cm buried in the sediments and 12 cm submerged in the water). Canopies covered 3 m in the stream-wise direction of the flume and extended halfway into the lateral side.

Two sand blockers positioned on either side of the canopies were employed to contain the sediments. The median grain size of the sample sands d_{50} is 0.5 mm.

The characteristics of turbulence influenced by the presence of canopies were quantified using ADV. Sediment scours around plants were captured by an RGB-D camera and the marked scales on the cylinders.

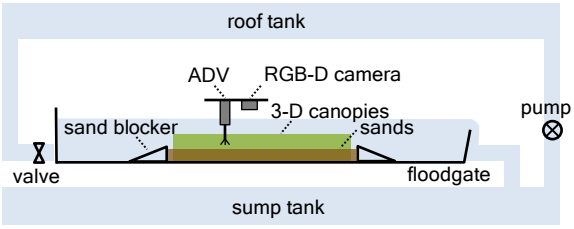

Figure 1 - Experimental set-up

NUMERICAL MODELING

An in-house code, CgLES-IBM (Complex Geometry Large Eddy Simulation-Immersed Boundary Method), was applied in numerical simulations. This model has been successfully applied in many engineering turbulence simulations (Chen et al., 2015; Ji et al., 2018). The governing equations of the incompressible flow are the spatially filtered Navier-Stokes equation and the continuity equation. The geometry of the solid surface was simulated by immersed boundary points (IBP), which was first introduced by Peskin (1972) in his simulations of the blood flow around the flexible leaflet of a human heart.

Periodical boundaries were adopted in the flow direction with a slope of $S = 0.005$ driving the fluid for full development. A non-slippery boundary was applied in the bottom boundary to reduce the near bed meshes. Slippery boundaries were used in the cross-sectional boundaries and the top boundary. The hydraulic conditions and vegetation parameters were maintained consistent with the experimental setups.

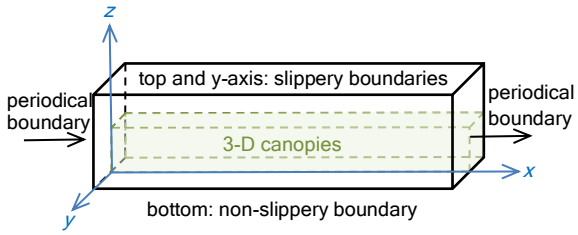

Figure 2 - Computational domain and boundary conditions

REFERENCES

Seddon, Chausson, Berry, Girardin, Smith, Turner (2020): Understanding the value and limits of nature-based solutions to climate change and other global challenges. Philosophical Transactions of the Royal Society B, vol. 375, pp. 20190120.

Nepf (2012): Flow and transport in regions with aquatic vegetation. Annual review of fluid mechanics, vol. 44, pp. 123-142.

Lei, Nepf (2021): Evolution of flow velocity from the leading edge of 2-d and 3-d submerged canopies. Journal of Fluid Mechanics, vol. 916: A36.

Kim, Kimura, Park (2018): Numerical simulation of flow and suspended sediment deposition within and around a circular patch of vegetation on a rigid bed. Water Resources Research, vol. 54(10), pp. 7231-7251.

Västilä, Järvelä (2018): Characterizing natural riparian vegetation for modeling of flow and suspended sediment transport. Journal of Soils and Sediments, vol. 18, pp. 3114-3130.

Zhang, Lei, Huai, Nepf (2020): Turbulence and particle deposition under steady flow along a submerged seagrass meadow. Journal of Geophysical Research: Oceans, vol. 125(5): e2019JC015985.

Chew, Nazarian, Norford (2017): Pedestrian-level urban wind flow enhancement with wind catchers. Atmosphere, vol. 8(9), pp. 159.

Peskin (1972): Flow patterns around heart valves: a digital computer method for solving the equations of motion [Ph. D. thesis]. Yeshiva University, New York.

Ji, Munjiza, Williams (2012): A novel iterative direct-forcing immersed boundary method and its finite volume applications. Journal of Computational Physics, vol. 231(4), pp. 1797-1821.

Chen, Ji, Wang, Xu, Campbell (2015): Flow-induced vibrations of two side-by-side circular cylinders: Asymmetric vibration, symmetry hysteresis and near-wake patterns. Ocean Engineering, vol. 110, pp. 244-257.